Recognition of Fiducial Surfaces in Lidar Surveys of Coastal Topography

John C. Brock, Asbury H. Sallenger, William B. Krabill, Robert N. Swift, and C. Wayne Wright

Abstract

A new method for the recognition and mapping of surfaces in coastal landscapes that provide accurate and low variability topographic measurements with respect to airborne lidar surveys is described and demonstrated in this paper. Such surfaces are herein termed "fiducial" because they can represent reference baseline morphology in studies of coastal change due to natural or anthropogenic causes. Non-fiducial surfaces may also be identified in each separate lidar survey to be used in a given geomorphic change analysis. Sites that are non-fiducial in either or both lidar surveys that bracket the time period under investigation may be excluded from consideration in subsequent calculations of survey-to-survey elevation differences to eliminate spurious indications of landscape change. This new analysis method, or lidar fiducial surface recognition (LFSR) algorithm, is intended to more fully enable the non-ambiguous use of topographic lidar in a range of coastal investigations. The LFSR algorithm may be widely applied, because it is based solely on the information inherent in the USGS/NASA/NOAA airborne topographic lidar coverage that exists for most of the contiguous U.S. coastline.

Introduction

Unlike passive optical sensors, lidars (**li**ght **d**etection **a**nd **r**anging sensors) that can fully resolve reflected laser waveforms have the capability to measure the vertical distribution of plant material (Blair *et al.*, 1994; Blair *et al.*, 1999; Lefsky *et al.*, 1999a; Lefsky *et al.*, 1999b; Means *et al.*, 1999), in addition to determining underlying ground elevations, also called "bald earth" topography (Krabill *et al.*, 1984; Ritchie, 1995; Kraus and Pfeifer, 1998). Most generally, "bald earth" refers to an imaginary land surface that has been stripped of all human construction, such as buildings and bridges, and also denuded of surface vegetation. The mapping of bald earth topographic surfaces through lidar surveys is of significant potential value in the interpretation of surficial geologic structure, in the modeling of fluvial runoff and storm surge inundation, in regional evaluations of land subsidence, and in assessing geomorphic change (Huising and Vaessen, 1997; Hampton *et al.*, 1999; Brock *et al.*, in press).

During the last few years, several research groups have in combination collected voluminous airborne laser observations along significant portions of the U.S. East, Gulf, and West Coasts (Carter and Shrestha, 1997; Gutelius *et al.*, 1997; Gutierrez *et al.*, 1998; Sallenger *et al.*, 1999; Krabill *et al.*, 2000). In particular, a cooperative program between the USGS, NASA, and NOAA has completed numerous airborne laser surveys using the NASA Airborne Topographic Mapper (ATM). In total, these topographic lidar surveys have covered roughly three quarters of the contiguous U.S. coastline since 1996, with repetitive coverage along substantial coastal reaches on the U.S. East and West Coasts (Brock *et al.*, 1999; Sallenger *et al.*, 1999).

A complication exists in exploiting the extensive coastal U.S. topographic lidar data set that has been collected thus far by the USGS/NASA/NOAA cooperative project beyond bare sand beachfaces, dunes, and overwash deposits. Elsewhere, if vegetation of significant height is present, it will reflect a portion of the laser energy, resulting in highly variable lidar elevation measurements that correspond to points at the top or within the vegetation volume, rather than the local ground level. Such effects may be considered to be a contamination of the true bald earth topography, but are also likely to provide unique information regarding the vertical structure of the vegetation canopy encountered by the laser pulses (Blair *et al.*, 1999).

In studies of geomorphic change based on the comparison of two or more lidar surveys over the same area that are separated in time, these vegetation effects will result in the depiction of elevation changes that are entirely an artifact of the lidar mapping method. The resulting elevation change maps will depict both *real* landscape alteration that has taken place during the time between the two surveys, and also *false* indications of landscape alteration that stem from the highly variable reflection of laser pulses from some types of vegetation.

If the goal is to simply detect morphologic change in coastal landscapes that has occurred between two lidar surveys, the strict determination of "bald earth" topography is not required. Rather, the requirement in this case is to recognize and capture topography over surfaces that yield consistent lidar elevation retrievals given no alteration between consecutive surveys. We herein define such surfaces as "fiducial," a word that means "taken as standard of reference" (Mish, 1989), and that is used in a similar context to describe reference marks placed on borders of geometrically controlled aerial photographs. Naturally occurring bald earth surfaces, for example, beachfaces, bare sand dunes, or ice sheets, are inherently fiducial. Should such a surface actually change in height during the time between two surveys but remain fiducial in character, the resulting perceived elevation difference may be regarded as *real* if it exceeds twice the known uncertainty in the lidar system's overall vertical accuracy. Thus, for fiducial surfaces such

J.C. Brock and A.H. Sallenger are with the USGS Center for Coastal Geology, 600 4th Street South, St. Petersburg, FL 33701 (jbrock@usgs.gov) (asallenger@usgs.gov).

W.B. Krabill and C.W. Wright are with the NASA Goddard Space Flight Center, Wallops Flight Facility, Wallops Island, VA 23337 (krabill@osb1.wff.nasa.gov) (wright@osb.wff.nasa.gov).

R.N. Swift is with EG&G, NASA Goddard Space Flight Center, Wallops Flight Facility, Wallops Island, VA 23337 (swift@aol5.wff.nasa.gov).

Photogrammetric Engineering & Remote Sensing
Vol. 67, No. 11, November 2001, pp. 1245–1258.

0099-1112/01/6711–1245$3.00/0

as beaches and dunes that are typically immediately adjacent to shorelines, elevation change determined by repetitive lidar surveys may be regarded as a true representation of actual geomorphic alteration, typically due to storm or eolian processes. The ocean surface is fiducial because at any instant in time the water surface is a sharp interface for laser reflection. Therefore, airborne topographic lidar may be used for mapping the water surface, but, due to constant variation under the influence of tides and waves, the ocean surface is not usually the subject of "change detection" studies based on repetitive lidar surveys.

Surfaces that result in variable lidar elevation retrievals given no *real* alteration between separate surveys are defined as non-fiducial, and result in *false* or spurious indications of landscape change when repeat lidar surveys are differenced. Although water surfaces may easily be masked in coastal lidar surveys based on the screening of low elevations and knowledge of tidal stage during the survey, the identification of landscape surfaces that are non-fiducial due to certain types of vegetation is less clearcut. First, the introduction of vegetation onto coastal land may result in either a fiducial or non-fiducial surface, depending on the density and species composition of the vegetation, also known as the community structure. Second, the design of the lidar instrument determines to some extent the increase in elevation error and variability introduced by various plant communities. In the case of the NASA ATM sensor (Krabill *et al.*, 2000), divergence from bald earth topography in surveys over vegetated areas is to be expected, because the design of this topographic lidar supports the capture of only the first reflection received for each laser shot that exceeds a predefined amplitude threshold. At any such location, the divergence from ground-level elevation caused by a static vegetation canopy will not necessarily be equivalent in multiple lidar surveys. This is because the vegetation canopy is a three-dimensional zone of many reflecting facets for laser energy whose structure varies rapidly with geographic location, and the exact laser ground spot locations are not identical between surveys.

Although simultaneous multispectral scanning would enable rapid identification of vegetative land cover based on the high near-infrared reflectance of most plants, it would not, however, be a panacea enabling the recognition of vegetation that is non-fiducial with respect to lidar elevation measurements. Based solely on passive spectral signatures, it would be difficult to universally separate dense, ground-level plants of less than 10 centimeters height that have no significant effect on lidar-based elevations (Krabill *et al.*, 2000) from vertically structured plant communities that do induce divergence of lidar-measured elevations from "bald earth" topography (McDonald *et al.*, 1998; Blackburn and Steele, 1999).

Objectives

Given the complications introduced by vegetation and a prime focus on sedimentary processes, most coastal research using topographic lidar to date has concentrated on shoreline, beachface, and headland change in response to wave action (Hampton *et al.*, 1999; Sallenger *et al.*, 1999). Detection of coastal landscape change on a national scale through complete use of the USGS/NASA/NOAA baseline topographic lidar data set requires that fiducial surfaces be identified wherever present within the entire surveyed area, a roughly 700-meter-wide strip that covers most of the contiguous U.S. coastline at the present time. Also, accurate topography of dunes landward of the beachface that may have varying levels of vegetative cover is required by new storm response models that seek to predict changes to barrier islands induced by hurricanes and other severe storms (Sallenger *et al.*, 1999; Sallenger, 2000; Morton, in press).

The goal of this paper is to present a method for the recognition of surfaces within coastal landscapes that are fiducial with respect to topographic lidar surveys, and thereby to more fully enable the use of topographic lidar in a range of coastal

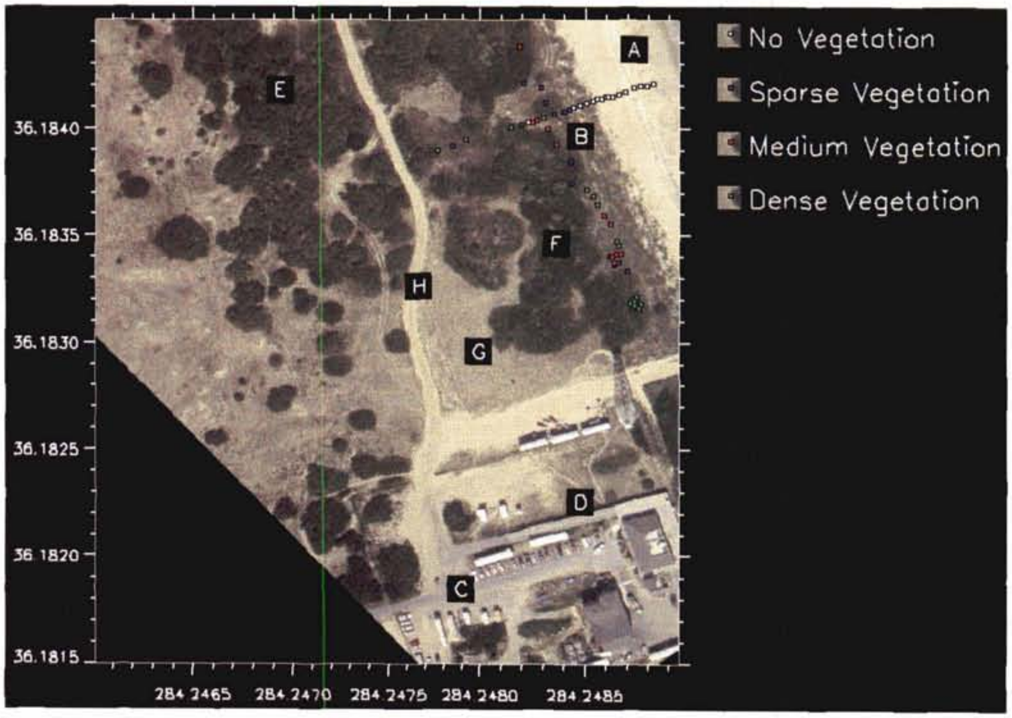

Plate 1. Vertical true color orthophotograph of Duck study area.

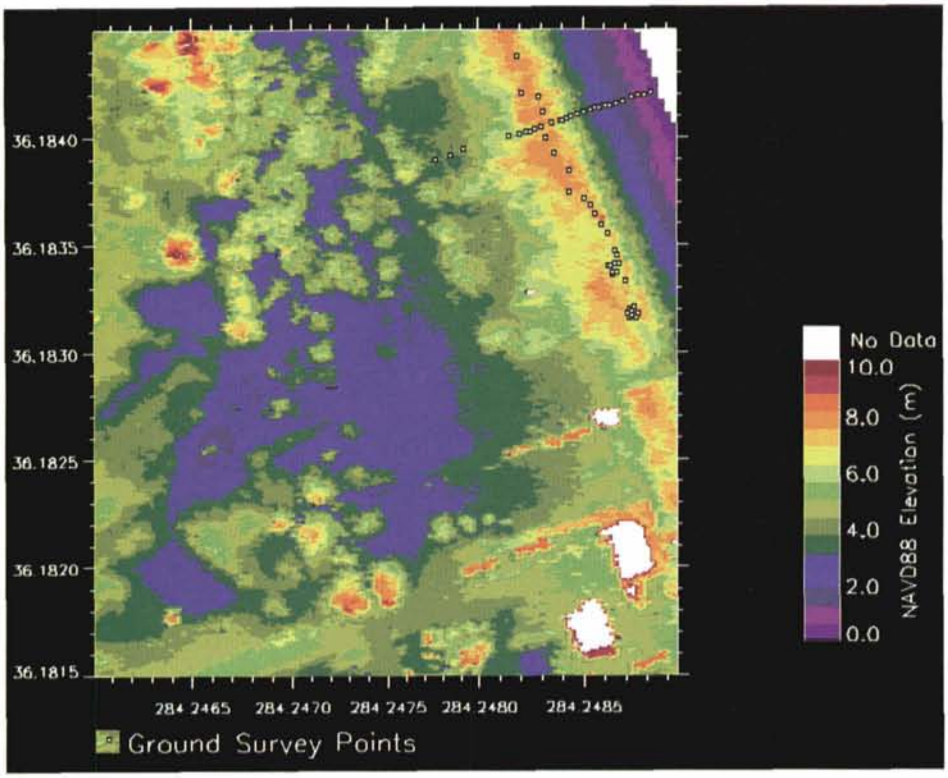

(a)

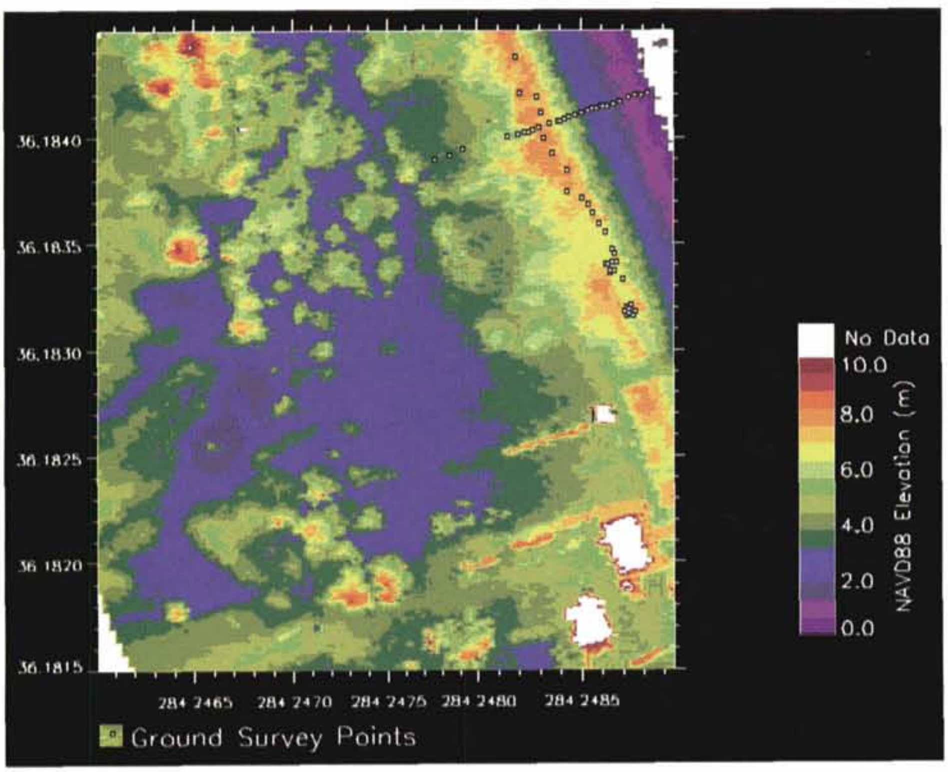

(b)

Plate 2. (a) NAVD88 elevation map for the Duck study area based on the NASA ATM lidar survey conducted on 26 September 1997. (b) NAVD88 elevation map for the Duck study area based on the NASA ATM lidar survey conducted on 27 September 1997.

investigations. The primary objective is to describe an algorithm that (1) maps areas that are fiducial for lidar elevation measurement, and (2) that is based solely on the information inherent in the laser backscatter and elevation measurements provided by most lidar systems, independent of ancillary imagery or ground surveys. A second objective is to demonstrate the performance of this algorithm within a test site on the North Carolina Outer Banks around the U.S. Army Corps of Engineers Duck Field Research Facility.

Field Methods

SandyDuck '97, a major field experiment, was carried out in the vicinity of the Corps of Engineers Field Research Facility (FRF) at Duck on the Outer Banks of North Carolina in the fall of 1997. Numerous participating investigators used ground-based systems to acquire highly accurate nearshore bathymetric and topographic measurements during SandyDuck '97, and aerial surveys acquired both low altitude vertical photography and two sets of dense topographic lidar observations. Accordingly, the SandyDuck '97 Experiment provides an excellent opportunity to closely examine the performance of lidar over diverse coastal land-cover types.

Aerial Photography

Vertical true color and near-infrared aerial photography were acquired by the USGS Coastal Aerial Mapping System (Hapke and Richmond, 2000) along 10-kilometer-long flightlines centered over the Duck, North Carolina Corps of Engineers FRF Research Pier during the SandyDuck '97 Experiment (Hapke and Richmond, 1999). The locations of ground control points that are easily identifiable in the photographs were surveyed using GPS equipment, and were used to georectify the photography. Subsequently, the exact region used for lidar algorithm development was subset from the resulting orthophotographs.

Topographic Lidar Observations

The NASA ATM topographic lidar was mounted on a NOAA Twin Otter aircraft and used to survey the Duck FRF study site during the SandyDuck '97 Experiment on two consecutive days, 26 September and 27 September 1997. The resulting data sets were each processed identically to yield one-meter gridded models of (1) NAVD88 elevation, (2) the maximum intensity of the laser backscatter associated with the laser ranging shots, and (3) the intensity of reflected panchromatic sunlight based on the ATM's passive light channel that collects observations between laser shots. The location of each laser shot reflected from the surface was determined by combining the laser range information with GPS-based aircraft position and aircraft attitude determined by an inertial navigation system (Krabill *et al.*, 2000). This procedure resulted in survey results expressed in IERS (International Earth Rotation Service) Terrestrial Reference Frame 1999 (ITRF99) coordinates, referenced to the WGS-84 ellipsoid.

Next, the ITRF99/WGS-84 elevation, backscattered sunlight, reflected laser intensity, and spot latitude and longitude position were extracted from each flightline data set that crossed the Duck FRF study site. The data set for each flightline was converted from its original conical scan geometry to an order in which consecutive point locations progress in latitude. The ITRF99/WGS-84 coordinates for the spot locations for each individual flightline were converted to the NAD-83 horizontal datum using the GRS-80 ellipsoid. Geoid height was calculated for each laser elevation measurement by use of the National Geodetic Survey's GEOID99 (J. Sonntag, personal communication) model, and the ellipsoid and geoid heights were summed to yield orthometric elevations in NAVD88, a vertical sea level datum (Zilkoski *et al.*, 1992). The geoid height and orthometric elevation calculations were not required for the reflected laser intensity and reflected sunlight data sets. The elevation, backscattered sunlight, and reflected laser intensity points for each separate flightline were merged into integrated data sets for the study site. Finally, a Delaunay triangulation for the 272-meter (east-west) by 301-meter (north-south) study region was performed on each variable's set of points. The resulting networks of triangles were then interpolated to create one-meter-resolution grids, and the gridded data sets were scaled to create images depicting NAVD88 elevation (meters), peak laser backscatter (relative units), and reflected sunlight (relative units). The one-meter-cell resolution used in gridding is on the order of the spatial density of the point data, which ranges within the surveyed area from more than one point per meter^2 to roughly one point per 2 meter^2.

Ground Survey Methods

Ground elevation was surveyed with total station equipment (T. Reiss, personal communication) along two orthogonal transects in the northeast portion of the Duck FRF study site on 30 September 1997, several days after the airborne lidar surveys. These control points were converted to geographic coordinates (latitude and longitude) for horizontal positioning, and to NAVD88 orthometric heights, to match the coordinate system used for the lidar spot elevations. Approximate vegetation height and density was recorded in four general classes at each of the topographic control points.

Results

Various landscape features are readily apparent on the true color aerial orthophotograph acquired over the Duck FRF study site (Plate 1). The beachface (Point A) and adjacent discontinuously vegetated primary dune (Point B) are seen in the northeast portion of the photograph. The landward edge of the swash zone lies at the extreme northeast corner of the study area. The COE Duck Field Research Facility buildings, parking lot (Points C and D), and antenna tower cover much of the photograph's southeast quadrant. The remainder of the scene depicts various oceanside shrub, intershrub, and planted Bitter Panicum/American Beachgrass plant communities (Points E, F, and G) that exist in the lee of the primary dune (Levy, 1976; Harris *et al.*, 1983). A north-south trending sand-surfaced unimproved road (Point H) bisects roughly the northern two-thirds of the orthophotograph.

The beachface, the primary dune and its landward swale, and the Duck FRF antenna tower and buildings are represented on elevation maps based on the NASA ATM lidar surveys conducted on 26 September and 27 September 1997 (Plates 2a and 2b). The cores of the taller Duck FRF structures are depicted as "No Data" regions because the analyzed lidar data range was restricted to 0 to 10 meters in order to scale the image map favorably for the depiction of natural landforms. Comparison of the histograms generated for each lidar survey (Figures 1a and 1b) reveals quite close, but not perfect, agreement between the elevations acquired on two consecutive days. Histogram regions separated by clear transitions in the elevation frequency distribution that correspond to the beachface (0 to 2 meters), the landward swale (2.5 to 5 meters), and the primary dune (6 to 9.5 meters) are depicted on these plots.

Laser backscatter for the 26 September 1997 survey varied across the study area in response to changes in land cover (Plate 3a), as did the intensity of reflected panchromatic sunlight (Plate 3b). Based on a visual comparison with the true color orthophotograph, the laser backscatter appears to be highly correlated with apparent vegetation density. In the vicinity of Point B, it appears that tall beach grasses growing on the foredune cast a shadow oceanward on the solar backscatter image. The lidar instrument itself serves as the illumination source for the laser backscatter image, and as a result this zone of foredune beach grasses does not create a laser shadow, but

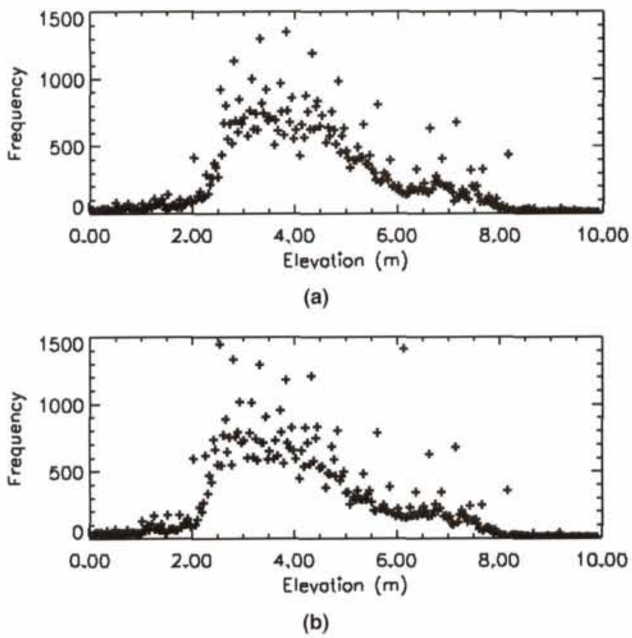

Figure 1. (a) Histogram of elevations for the Duck study area based on the NASA ATM lidar survey conducted on 26 September 1997. (b) Histogram of elevations for the Duck study area based on the NASA ATM lidar survey conducted on 27 September 1997.

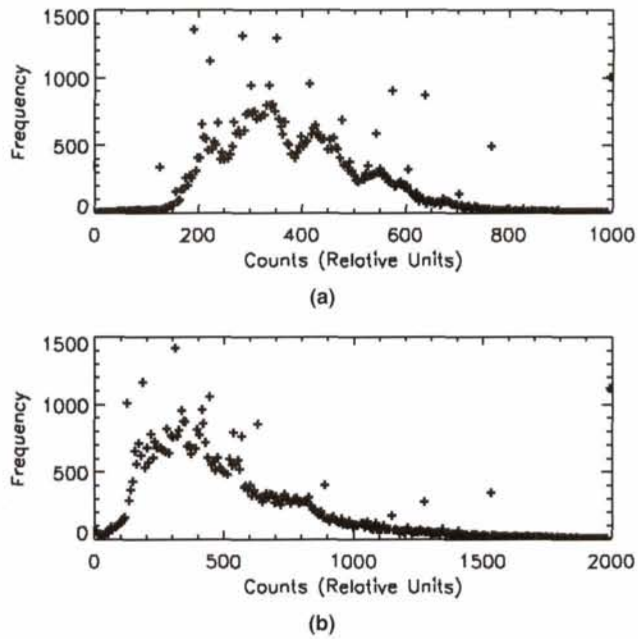

Figure 2. (a) Histogram of the peak laser backscatter values for laser shots over the Duck study area acquired by the NASA ATM lidar survey conducted on 26 September 1997. (b) Histogram of the reflected panchromatic sunlight values for spots between the laser shots over the Duck study area acquired by the NASA ATM lidar survey conducted on 26 September 1997.

does appear to slightly decrease the amplitude of the reflected laser pulses. A histogram for laser backscatter (Figure 2a) depicts several pronounced peaks and troughs that are not apparent on the histogram for panchromatic reflected sunlight (Figure 2b). This suggests that laser backscatter variation is superior to changes in passive channel brightness in resolving diverse land-cover classes and their boundaries.

The vegetation at each topographic control point along the 30 September 1997 elevation survey was assigned to one of four classes defined by a qualitative appraisal of plant cover density. The vegetation class definitions are (1) no vegetation, (2) sparse vegetation, (3) vegetation of medium density, and (4) dense vegetation. The ground survey observations were not sufficiently quantitative with regard to plant community species and geometry to allow their rigorous use in lidar algorithm creation, but do illustrate trends in topographic lidar performance with changes in vegetation characteristics. The ground survey results are useful in assessing in a general sense the impact of varying vegetation on the peak amplitude of reflected laser brightness, on the intensity of broad visible band solar reflectance, and on the reliability and repeatability of lidar elevation measurements.

The ground survey consists of two roughly orthogonal transects that intersect near the crest of the primary dune (Plates 1 and 2a). The first transect is 108 m long, and extends northeast to southwest from a point on the beachface just above the swash zone landward over the primary dune, and into a backdune area covered by beachgrass, intershrub, and shrub. The density and height of the backdune vegetation generally increases with distance from the primary dune crest. The second transect traces the northwest to southeast trending primary dune crest for about 136 meters. This transect mostly crossed sandy terrain vegetated by sea oats and other beach grasses, but locally encountered clumps of denser vegetation.

Based on extreme differences between the vegetation cover maps produced in 1976 (Levy, 1976) and in 1983 (Harris *et al.*, 1983), it is clear that vegetation at the Duck FRF site has recently undergone rapid evolution. However, comparison of our 1997 field observations with the detailed descriptions provided 15 years earlier by Harris *et al.* (1983) allows us to relate our simple vegetation classes to the plant communities recognized by these earlier researchers. Our Sparse Class appears to be mostly planted American beachgrass (*Ammophila beviligulata*) mixed with sea oats (*Uniola paniculata*) and bare sand, the Medium Class is typically American beachgrass interspersed with oceanside intershrub (*Bitter panicum*), and the Dense Class is apparently dominated by oceanside shrub. As can be seen by inspection of the true color orthophotograph, the shorenormal transect did not extend far enough westward to encounter the study site's densest and highest vegetation, mostly located west of the north-south sandy road.

The presence of vegetation increased the mean difference between the lidar and ground survey elevations from a minimum of 0.26 meters over bare sand to values near 0.4 meters for all vegetated classes (Figure 3a and Table 1). The increase in the variance of the lidar to ground survey elevation difference was much more pronounced, rising from 0.03 meters for bare sand to a high of 0.27 for sparsely vegetated sand. In terms of both variables, the poorest lidar to ground survey agreement in elevation occurred for the Sparse Class.

Comparison of laser backscatter to vegetation class (Figure 3b and Table 1) reveals that the peak laser backscatter recorded by the ATM drops as vegetation density and height increases. This effect is also readily apparent in a qualitative sense through comparison of the true color aerial orthophotograph (Plate 1) and the laser backscatter image map (Plate 3a) for the study site. The laser backscatter map shows that the highest laser backscatter comes from sandy surfaces, breaking waves, and the light colored portion of the Duck FRF building roof.

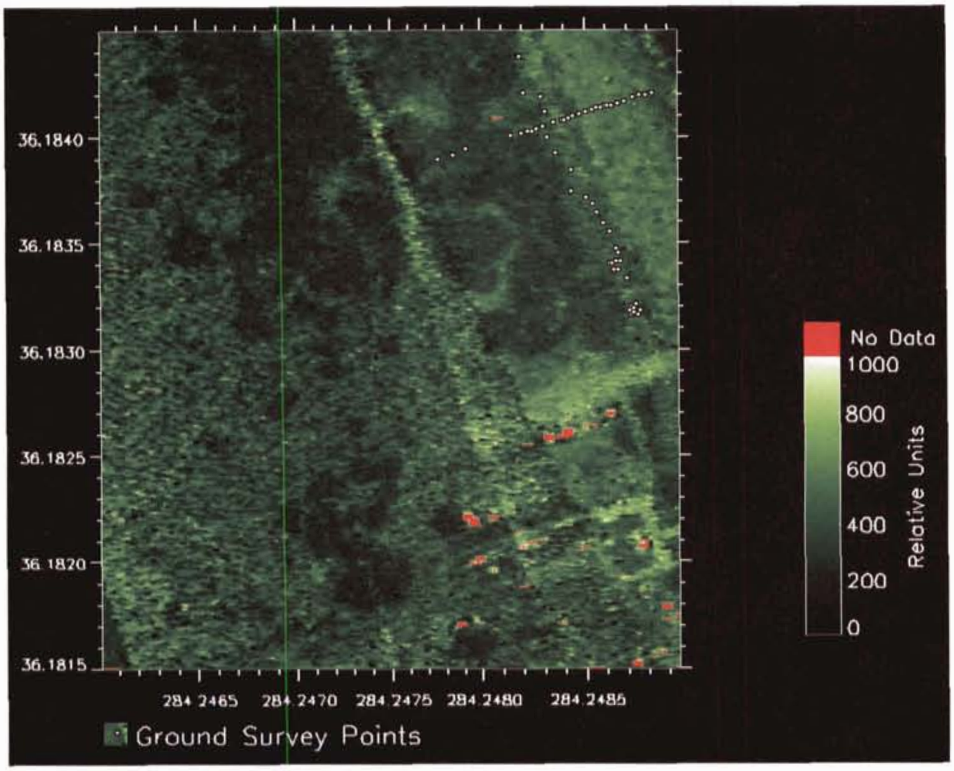

(a)

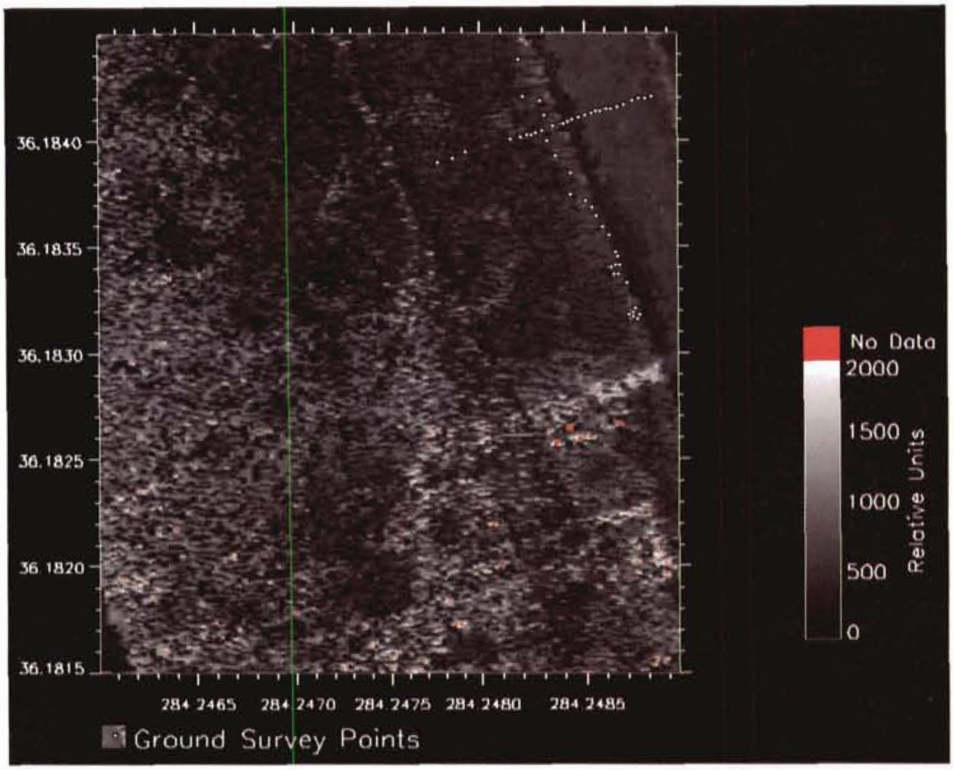

(b)

Plate 3. (a) Laser backscatter map for the Duck study area based on the NASA ATM lidar survey conducted on 26 September 1997. (b) Map depicting the intensity of reflected panchromatic sunlight for the Duck study area based on the NASA ATM lidar survey conducted on 26 September 1997.

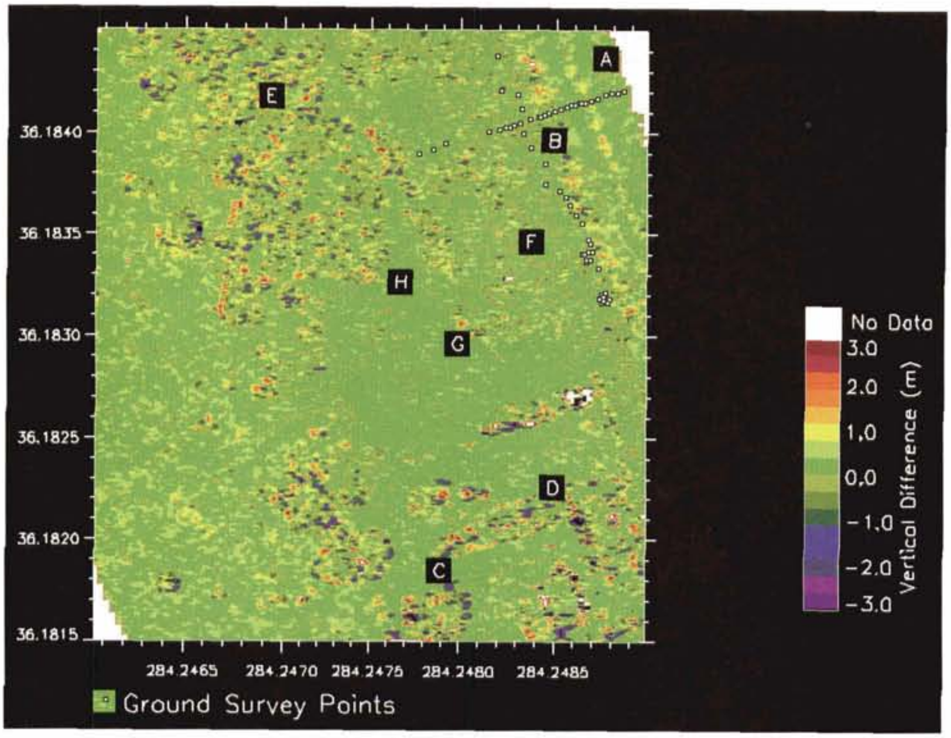

Plate 4. Map depicting the difference between the NAVD88 elevation maps for the Duck study area based on NASA ATM lidar surveys conducted on 26 September 1997 and 27 September 1997.

Dark regions on the laser backscatter map mostly correspond to dense, tall vegetation and to wet areas within the swash zone.

Fiducial Surface Recognition Algorithm

Spatial Variation in Laser Backscatter

Two hypotheses may be offered to explain the observation that laser backscatter in general decreases with increasing vegetation density and height within the study site. First, the spectral reflectance of vegetation at green wavelengths is much less than that of bare sand, which has extremely high reflectance throughout the visible spectrum. Laser reflections from areas with some plant cover drop relative to bare sandy surfaces because a portion of the illuminated laser spot has a lower green reflectance. A second reason relates to the more extreme decrease in laser backscatter observed within the taller shrubs and small trees that are mostly found in the western half of the study area. Based on previous research on the interaction of lidar pulses with vegetation canopies (Blair *et al.*, 1994; Blair *et al.*, 1999; Lefsky *et al.*, 1999a; Lefsky *et al.*, 1999b; Means *et al.*, 1999), we infer that the plant communities at these locations act as a vertically inhomogeneous reflecting layer composed of a myriad of branches and leaves that act as a population of reflecting facets. This results in multiple reflections from a single laser shot that spread out the reflected laser energy into many small peaks in the reflected waveform. In contrast, a dry beachface not only has a high green reflectance, but also acts as a single discrete reflector that concentrates the bulk of the reflected laser power into a single peak.

Spatial Variation in the Consistency of Lidar Elevation Retrieval

We assume that virtually no real change in landscape morphology occurred within the Duck study site between the surveys on 26 September 1997 and 27 September 1997, aside from highly localized and easily identifiable changes in the beachface due to wave action during the intervening day, and variation in the distribution of cars and trucks in the Duck FRF parking lot. However, inspection of the elevation histograms for these two surveys reveals some differences (Figures 1a and 1b). Beachface erosion or accretion would cause minor histogram disagreement at very low elevations near mean sea level, but the most obvious lidar survey-to-survey disagreement seen on the elevation histograms occurs in the 2- to 4-meter NAVD88 height range. The spatial pattern of this disagreement was investigated by differencing the lidar elevation maps generated separately from the 26 September 1997 and the 27 September 1997 lidar surveys (Plates 2a and 2b). Comparison of the resulting lidar elevation difference map (Plate 4) to the coregistered true color orthophotograph (Plate 1) reveals that the most extensive survey-to-survey disagreement in elevation occurred at the most heavily vegetated sites (for example, Point E), which we infer to have undergone no actual change in the one day that elapsed between the two surveys. We believe that the high variability of apparent lidar elevations within heavily vegetated areas was caused by the unique and inconsistent interaction of each survey's individual laser shots with this highly complex landscape boundary. We infer that minor differences in the ensemble of laser shot ground locations and incidences angles between the surveys resulted in differences in the multiple reflecting facet populations of leaves and branches encountered by each survey's collection of laser shots in the study area, and that this effect caused the apparent elevation differences.

Other sites of lidar survey-to-survey disagreement occur about the Duck FRF facilities (Points C and D), and in two shore-parallel linear trends on the beachface (Point A) and on the steep foreslope of the primary dune (Point B). The spotty, nar-

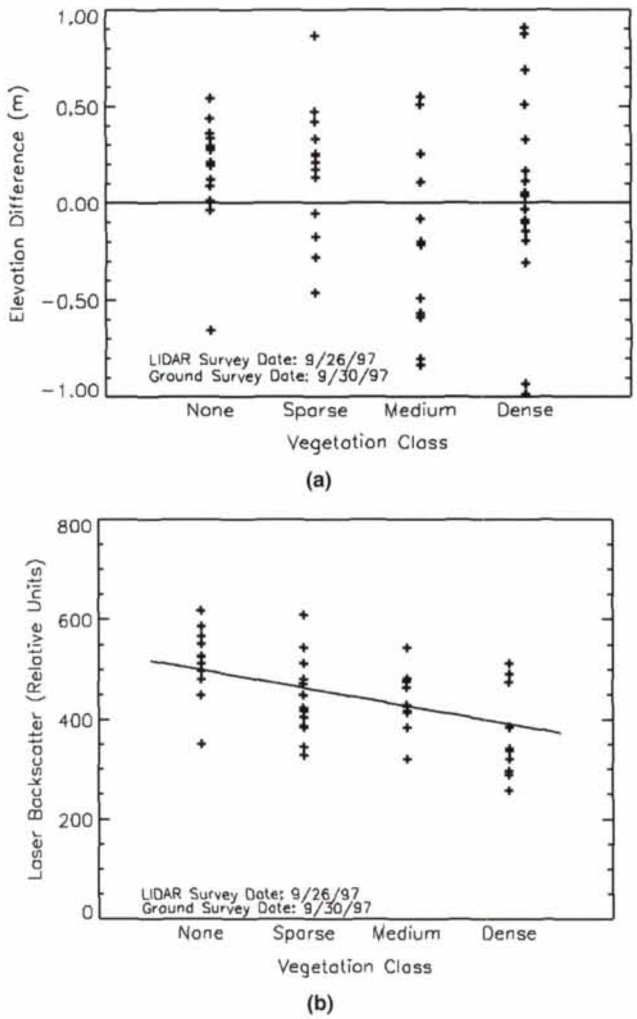

Figure 3. (a) Scatterplot of the difference between 26 September 1997 lidar survey elevations and collocated ground survey elevations, grouped by vegetation class. (b) Scatterplot of the peak laser backscatter for the 26 September 1997 lidar survey at ground survey locations, grouped by vegetation class.

row zone of elevation differences at Point A on the beachface may be due to actual geomorphic change, because this surface was likely exposed to wave action during the short time period bracketed by the two lidar surveys. Similarly, some of the elevation change seen about the Duck FRF parking lot is probably due to alteration in the distribution of parked cars and trucks, and therefore represents real landscape variation. Other apparent elevation change about the Duck FRF buildings may have arise due to slight horizontal positioning errors in the vicinity of extreme topographic slopes, such as are created by the vertical sides of buildings and other human constructions. Along the edge of a rooftop, for example, minor disagreement in survey-to-survey position can result in spurious indications of extreme change in elevation. This same effect may have caused the apparent elevation differences along the steep foreslope of the primary dune (Point B), and in addition, some of the disagreement in this zone may be due to the presence of dense clumps of sea oats and other beach grasses. Given the role of dunes in defining shoreline relief, and the importance placed on dune height and morphology within storm impact models, the accuracy of lidar topographic surveys of coastal dunes, and any unique error sources in lidar elevation measurement caused by the morphology or characteristic plants of these landforms, requires further examination. A comparison of lidar elevation measurements to total station elevations along the transect that follows the dune crest showed a mean disagreement in elevation of 0.441 meters. Given that this transect traversed various vegetation classes commonly found on southeastern U.S. coastal dunes, bulk disagreements in lidar-to-ground survey elevation of this general magnitude are expected elsewhere for vegetated dunes in similar settings.

Criteria for the Recognition of Discrete Laser Reflectors

The "discrete" reflection of laser energy is a prime characteristic of simple surfaces that are fiducial for laser elevation surveys, and this concept is the basis for the algorithm proposed herein for the recognition of surfaces that are fiducial with respect to lidar elevation measurements. Discrete reflectors are composed of a single sharp reflecting surface for laser energy that results in highly consistent and repeatable lidar elevation retrievals. For example, a sandy beach, a parking lot, or a field covered with short grass are likely to act as discrete reflectors. A discrete reflector is not necessarily a natural surface, nor must it be free of vegetation, as is the case for a bald earth surface. As such, a discrete reflector does not necessarily have a passive spectral signature that would signify soil or surficial sediment, and may even have a spectral signature for reflected sunlight that is characteristic of healthy or senescent vegetation, or in the case of a roof top, paint pigment, or tar. Vegetation that has vertical heterogeneity due to a canopy structure, or even a single story with significant volume, is probably the primary type of non-discrete reflector that occurs within coastal landscapes.

A second criterion for a discrete reflector incorporated in our fiducial surface identification method is that, over such surfaces, the accuracy and reliability of elevation retrieval is not a function of laser reflectance. Consider that, across a beach that grades from wet to dry, the wet portion of the beach will have a lower green laser reflectance than will the dry beach, but there will be no variation in the elevation retrieval accuracy and repeatability between the wet and dry beach. Alternatively, consider a complex vegetation canopy, in which changes in the three-dimensional distribution of reflecting facets will cause both the peak amplitude of the reflected waveform and the apparent laser range to vary over small spatial scales. In the design of the lidar fiducial surface recognition algorithm that we propose, the peak of the backscattered laser waveform is

TABLE 1. LIDAR ELEVATION TO GROUND SURVEY ELEVATION COMPARISON

Vegetation Class	Mean of the Lidar to Ground Survey Elevation Difference (meters)	Variance of the Lidar to Ground Survey Elevation Difference (meters)	Mean Laser Backscatter (relative units)
None	0.263	0.034	510.5
Sparse	0.481	0.270	440.3
Medium	0.434	0.066	438.0
Dense	0.380	0.126	393.2

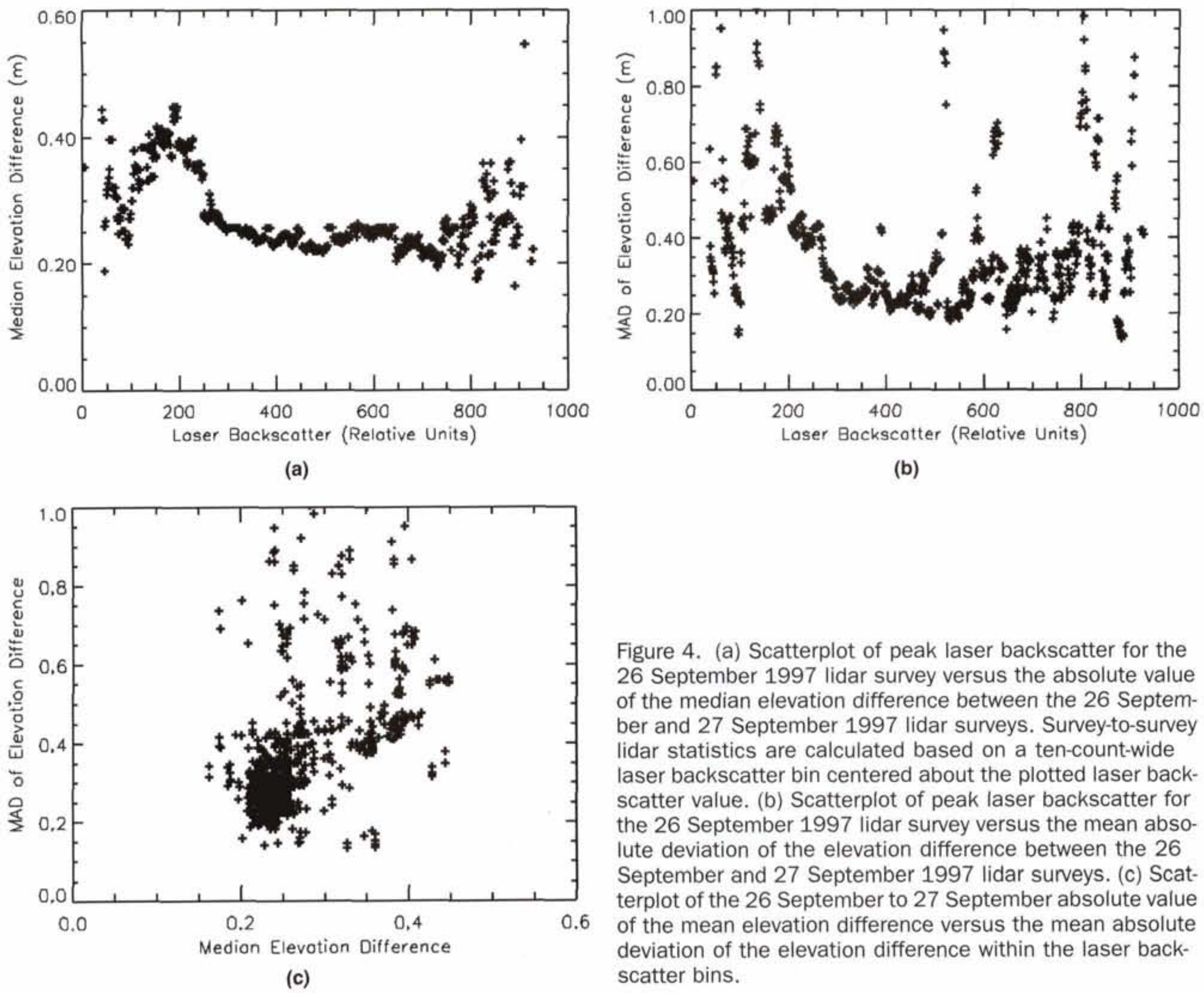

Figure 4. (a) Scatterplot of peak laser backscatter for the 26 September 1997 lidar survey versus the absolute value of the median elevation difference between the 26 September and 27 September 1997 lidar surveys. Survey-to-survey lidar statistics are calculated based on a ten-count-wide laser backscatter bin centered about the plotted laser backscatter value. (b) Scatterplot of peak laser backscatter for the 26 September 1997 lidar survey versus the mean absolute deviation of the elevation difference between the 26 September and 27 September 1997 lidar surveys. (c) Scatterplot of the 26 September to 27 September absolute value of the mean elevation difference versus the mean absolute deviation of the elevation difference within the laser backscatter bins.

used as a proxy for coastal landscape characteristics that control the "discreteness" of laser reflection.

Analysis of Reflector Characteristics within Laser Backscatter Bins

Application of the lidar fiducial surface recognition (LFSR) algorithm requires a training site that represents all of the landscape types within the coastal reach under analysis, and that has been surveyed twice by a topographic lidar within a very short time period, so that no real change has occurred. In our demonstration, the training site is equivalent to our entire study area, but in practice the algorithm training statistics developed for a restricted site would be used to extrapolate the classification of fiducial versus non-fiducial surfaces across a broad coastal reach. This coastal reach adjacent to the training site need only be surveyed with lidar once, and it's geographical extent is limited by two factors: the (1) drift in the calibration of the laser receiver, and (2) the appearance of landscape types that are not present in the training site.

The training site analysis begins with the creation of a lidar elevation difference map that depicts apparent change between the two surveys (Plate 4). Numerous coastal landscape subregions that display nearly identical peak laser backscatter are identified on the elevation difference map. The population of elevation difference values that corresponds to each short interval in laser backscatter range, or "bin," is used to calculate statistics that serve as metrics for the discreteness of laser reflection in that subregion. Elevation difference statistics were calculated for 995 map grid-cell populations within subregions defined by a sliding ten-count-wide laser backscatter bin that progressed at an increment of one count through the laser backscatter map range of 0 to 1000 (relative units). For each laser backscatter bin centerpoint, all of the laser backscatter map cells that fell into the ten-count-wide bin about that centerpoint where identified. Next, the elevation difference map-cell positions that corresponded to those same positions were flagged. Finally, for each of the 990 laser backscatter bins, the flagged elevation difference values for that bin were subjected to a statistical analysis to determine the nature of the reflector represented by that level of laser backscatter.

Recognition of Surfaces Composed of a Single Reflecting Facet

As discussed above, in determining elevations with lidar, a sharp single reflecting surface typically results in highly consistent elevation retrievals, and thus may be considered fiducial with respect to lidar techniques. In order to test for high repeatability of lidar elevation measurement, two statistics were calculated for each laser backscatter bin, the median elevation difference (MED) (Figure 4a), and the mean absolute deviation of the elevation difference (MADED) (Figure 4b). A very distinct pattern emerged for both MED and MADED versus laser

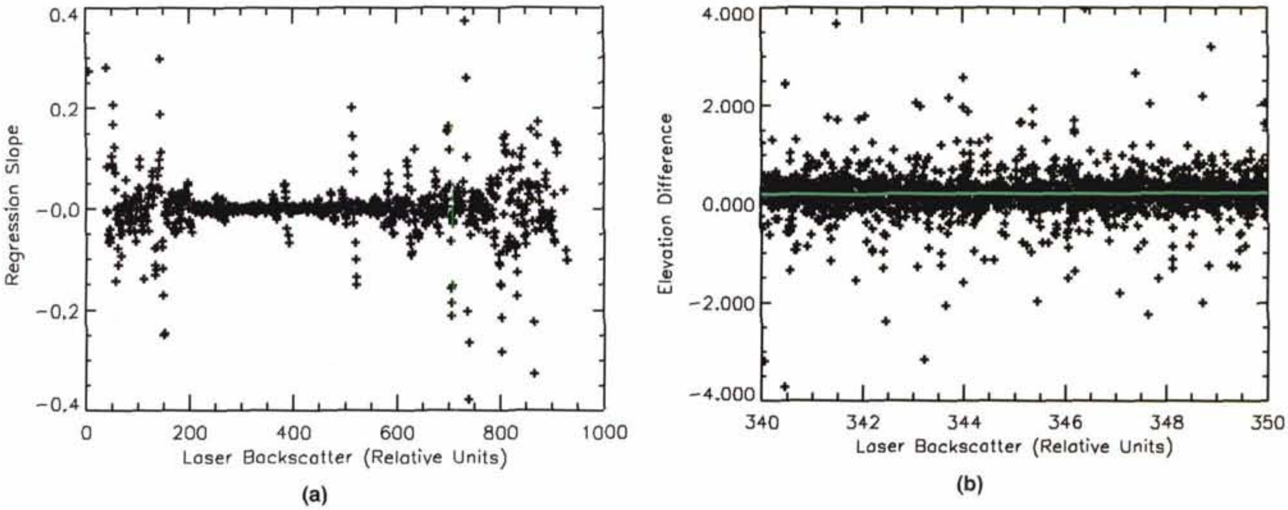

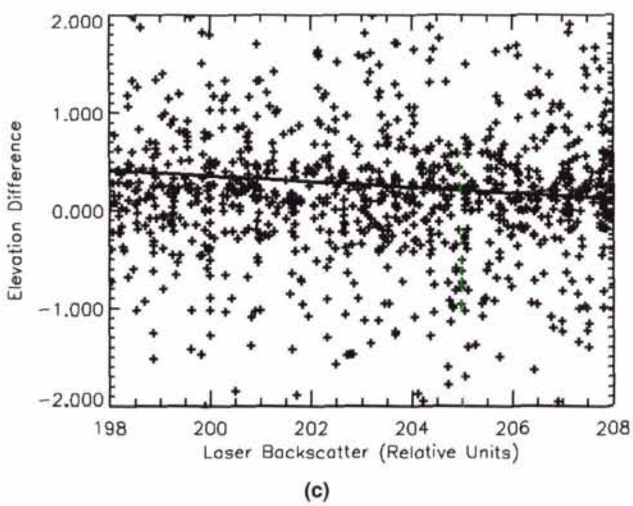

Plate 5. (a) Scatterplot of peak laser backscatter for the 26 September 1997 lidar survey versus the slope of the linear regression of laser backscatter to survey-to-survey elevation difference for grid cell populations the correspond to each ten-count-wide wide laser backscatter bin centered about the plotted laser backscatter value. (b) Scatterplot of peak laser backscatter versus survey-to-survey elevation difference for the laser backscatter bin centered at 345 relative units. The slope for this linear regression is nearly zero, evidence for a fiducial surface. (c) Scatterplot of peak laser backscatter versus survey-to-survey elevation difference for the laser backscatter bin centered at 203 relative units. The slope for this linear regression diverges significantly from zero, suggesting a non-fiducial surface.

backscatter, with both showing consistent and stable high repeatability of elevation measurement in the laser backscatter range from about 300 to 750 relative units. In this range, the MED is consistently near 25 cm, a reasonable result, given the 15-cm vertical accuracy expected for each individual survey (Krabill *et al.*, 2000). Furthermore, a scatterplot of MED versus MADED depicts a well defined cluster for the laser backscatter bins that yield the most repeatable lidar elevation measurements (Figure 4c). This result suggests that both MED and MADED degrade as a function of the same landscape characteristics, here captured by proxy through variation in laser backscatter. Elevation repeatability is severely degraded below laser backscatter values of 300 relative units. Inspection of the true color orthophotograph (Plate 1) and the laser backscatter image map (Plate 3a) together reveals that the corresponding geographic region is mostly covered by thick vegetation.

However, a simple MED or MADED versus laser backscatter thresholding algorithm for discrimination of discrete from non-discrete reflectors within the study area would be insufficient, because based on both MED and MADED, repeatability of elevation retrieval improved markedly around laser backscatter at 100 relative units to essentially match the performance in the 300 to 750 (relative units) laser brightness range. Accordingly, identification of non-discrete reflectors based on simple laser backscatter thresholding would contain obvious errors, because it would not distinguish cases in which depressed laser backscatter is due to a discrete reflector that has a low green laser reflectance, rather than being composed of multiple reflecting facets that result in decreased peak backscatter. Possible examples of such surfaces include wet beach, beaches comprised of mafic sand grains, asphalt roads and parking lots, and flat tar-covered building rooftops. The apparent high repeatability of elevation retrieval for such surfaces in the study area can be verified by comparing the true color orthophotograph (Plate 1) to the lidar elevation difference map (Plate 4). The repeatability of lidar elevation measurement over these relatively dark surfaces attests to the accuracy of the "range walk" calibration performed for the NASA ATM (Brock *et al.*, in press).

Recognition of High Decorrelation between Laser Reflectance and Lidar Elevation Repeatability

We have proposed two reasons for low laser backscatter from a given site within a coastal landscape: i.e., (1) the peak amplitude of the returned waveform is diminished by the occurrence of numerous reflecting facets within a vertically complex surface vegetation layer, and/or (2) the surface within the laser spot has low inherent green laser reflectance. Our LFSR algorithm requires that these two cases be distinguished, because the second case may include locations that are dark on a laser backscatter map, but that nonetheless act as fiducial surfaces with respect to lidar surveys. Our approach to making this second, more subtle, discrimination assumes that, for discrete reflectors, variation in laser reflectivity is nearly perfectly decorrelated with variation in the repeatability of laser ranging to yield

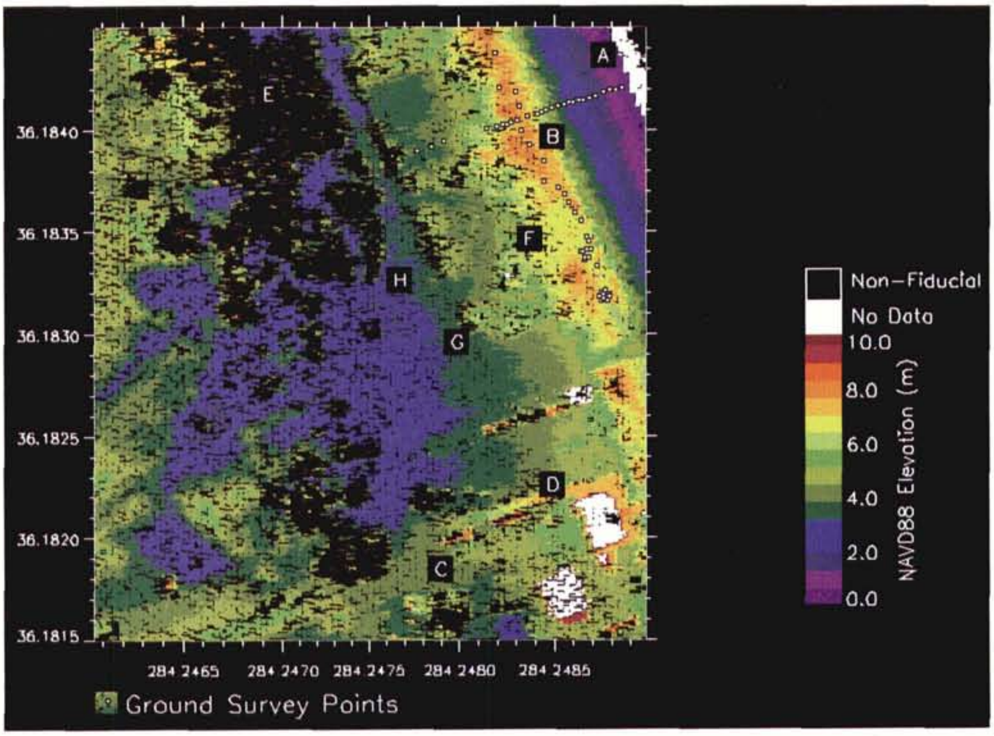

Plate 6. NAVD88 elevation map for the Duck study area based on the NASA ATM lidar survey conducted on 26 September 1997 that has been masked to represent only the topography of surfaces recognized as fiducial.

elevation. For example, the laser albedo of a beachface at low tide that grades laterally from wet to dry sand will vary with moisture content, but the repeatability of elevation measurements should be consistently high everywhere across this sharp air/terrain boundary. In such cases, a tight laser backscatter to elevation difference regression line fit at near zero slope, signifying maximum decorrelation, is anticipated. Alternatively, variation in laser brightness within dense vegetation may also be due to variation in the three-dimensional distribution of reflecting facets. In such cases, laser range will to some degree covary with backscatter, and this effect will degrade the decorrelation between laser brightness and survey-to-survey elevation difference that is characteristic of discretely reflecting surfaces. In order to admit this second criterion, the degree of decorrelation between laser reflectance laser elevation repeatability was determined by linear regressing laser backscatter against elevation difference within each of the 990 ten-count-wide laser brightness bins. The regression slope, herein used as an indicator of decorrelation, was found to display a distinctive pattern with respect to laser backscatter (Plate 5a), and is near zero (+0.0027) for the subregion defined by the laser backscatter bin centered at 345 (relative units), previously determined to be a discrete reflector based on MED and MADED (Plate 5b). In contrast, the linear regression for the laser backscatter bin centered at 203 (relative units), which based on its high MED and MADED is non-discrete, has a slope (−0.0297) that diverges somewhat from zero (Plate 5c).

LFSR Algorithm Decision Rule

The LFSR algorithm selects the laser backscatter bins that plot in a tight cluster at the apex of a cone-shaped cloud of points within an imaginary volume whose axes are laser backscatter bin MED, MADED, and regression slope (Figure 5). The laser backscatter bins that correspond to map subregions that reflect most discretely are concentrated in the apex cluster. A decision rule that defines membership in this cluster serves to separate map subregions classed as fiducial from those determined to be non-fiducial. Given a large enough training site, various types of non-fiducial surfaces may result in distinct clusters, beyond the fiducial surface apex cluster seen in our example. In such cases, an objective clustering analysis would be a viable method to assign membership to the fiducial surface cluster.

Given the lack of well defined non-fiducial clusters for our training site, we selected thresholds for laser backscatter bin MED, MADED, and regression slope to bracket the cluster that represents fiducial surfaces. Picking these thresholds is at this point somewhat subjective, but this may be desirable in some cases, because it allows the judgment of the interpreter, and the scientific goals of the specific lidar application, to play a role in fiducial surface classification. The criteria for a laser backscatter bin's corresponding subregion to be classed as fiducial that was entered into the LFSR algorithm is listed in Table 2.

This decision rule was applied only to laser backscatter bins with centerpoint values of 750 relative units or less, because laser backscatter bins with centerpoint values above 750 relative units appeared to be associated with bright speckle in the laser-based images, and represent only a minor fraction of the total number of map grid cells.

The LFSR algorithm was applied to the NASA ATM survey that was conducted on 26 September 1997, and enabled the masking of all non-fiducial surfaces in the resulting NAVD88 elevation map (Plate 6). Comparison of this elevation map with the true color orthophotograph verifies that obvious bare sandy surfaces (Point A) and the Duck FRF parking lot (Point C) are appropriately recognized as fiducial by the LFSR algorithm. As anticipated, the relatively tall and dense oceanside shrub west

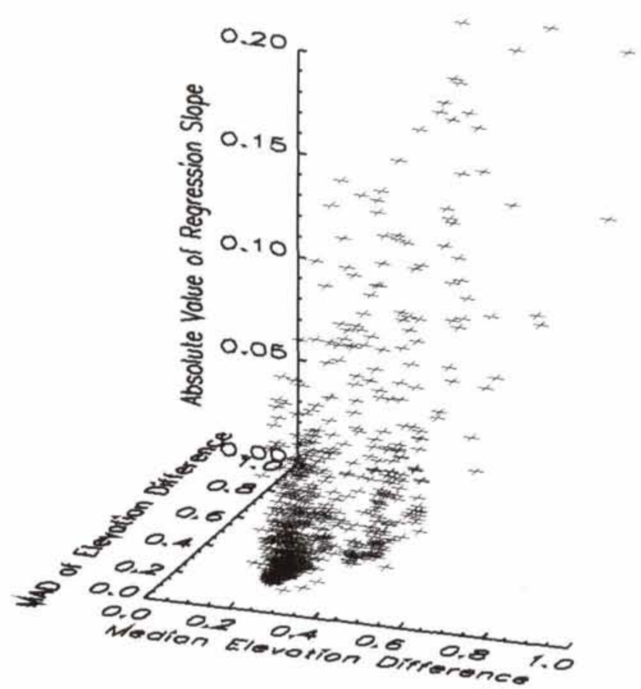

Figure 5. Three-dimensional scatterplot of ten-count-wide laser backscatter bins within a volume defined by the median elevation difference, mean absolute deviation of elevation difference, and laser backscatter to elevation difference corresponding to each bin.

of the north-south trending road (Point E) that splits the study site is nearly all classed as non-fiducial, and masked accordingly. Much of the shrub that exists to the east of the road in the lee of the primary dune (Point F) acts as a fiducial surface for laser ranging, as can be verified by inspection of the survey-to-survey elevation difference map (Plate 4) Nelson *et al.* (1984) found that forest canopy closure is strongly and inversely related to the penetration of laser pulses in dense vegetation, which suggests that the LFSR algorithm detected shorenormal gradation in shrub crown closure. Strong shorenormal gradients in the physical environment of barrier islands exist for a variety of factors such as wind velocity, sand movement, periodic flooding, and salt spray. These gradients are very steep close to the ocean, and strongly impact soil composition, nutrient fluxes, and plant stress and mortality (Ehrenfeld, 1990). Our results suggest that NASA ATM topographic lidar surveys may have some capability to recognize the variation in vegetation caused by strong environmental influences associated with barrier island environments.

At sites where spurious survey-to-survey elevation differences are due to horizontal error in point positioning about abrupt topographic steps, the LFSR algorithm may become unreliable. This results because survey-to-survey disagreement in

TABLE 2. DECISION CRITERIA FOR THE LFSR ALGORITHM

Laser Backscatter Metric	Minimum	Maximum
Median Elevation Difference	0 centimeters	30 centimeters (absolute value)
Mean Absolute Deviation of the Elevation Difference	0 centimeters	40 centimeters
Regression Slope	−0.05	+0.05

elevation due to edge mismatch is not associated with variation in laser backscatter, used by the LFSR algorithm to define subregions for classification. In our example, sites that may correspond to horizontal mismatch "halos" along the steep foredune (Point B) are classed as fiducial, but algorithm performance about the sides of the Duck FRF buildings (D) is less consistent. Masking within a geographical buffer about all regions in lidar elevation maps with slopes that exceed a threshold corresponding to the maximum acceptable vertical error caused by inaccuracy in horizontal positioning of laser shots would resolve this ambiguity in resolving coastal change through the differencing topographic lidar surveys.

A very restricted test area has been analyzed in this study to enable demonstration and visual verification of a new method for identifying surfaces that are fiducial with respect to NASA ATM topographic lidar elevation measurements. In practice, the resulting LFSR algorithm will only be of use within studies of coastal change if it is applied over extensive coastal reaches. This requires including within a broader coastal mapping program the repetitive surveying of training sites within short time periods on the order of one day or less, during which it can be assumed that no landscape change has occurred. Fortunately, such sites reside at the starting location for each the coastal reach mapped during the roughly 4-hour missions that summed together form the extensive lidar data set collected thus far by the USGS/NASA/NOAA coastal mapping project. Typically, about 200 kilometers per day of coastline is surveyed during a mapping mission, and operations are conducted to provide roughly a 50-kilometer-long coastal stretch of overlap at the beginning of each consecutive daily survey.

We propose the application of the LFSR algorithm within lidar-based assessments of large-scale coastal change in order to eliminate or reduce the spurious identification of false geomorphic change that is caused by the inclusion of non-fiducial vegetated terrain. Given a baseline topographic survey of an extensive coastal reach (>1000 kilometers) with the roughly 50 kilometers overlap between daily surveys described above, the application of this method would follow processing to create gridded elevation and laser backscatter surfaces. First, training sites within the daily overlap regions contained in the baseline survey extent would be selected and used to calibrate the LFSR algorithm for each daily mission. Non-fiducial surfaces would then be masked as such within the gridded elevation data sets collected on each day of the baseline survey. Topographic lidar data collected later following a storm impact would be subjected to an identical analysis, resulting in gridded elevation fields for both the pre- and post-event surveys that are masked for regions in which elevations are unreliable. Differencing of the topographic grids based on the two surveys to evaluate true geomorphic change would then be undertaken only for sites classified as fiducial in both surveys. The final topographic change map would only depict results for consistently fiducial areas, taken to represent real landscape change, largely free of apparent change introduced as an artifact of the laser sensing method.

Conclusions

The LFSR algorithm that we have described and demonstrated in this paper is designed to classify coastal landscape surfaces as either fiducial or non-fiducial with respect to topographic lidar surveying based on whether or not that surface reflects individual laser pulses in a discrete manner. Implicit in this approach is the assumption that discrete reflectors yield consistent laser range measurements in repeat lidar surveys. As defined here for the purposes of algorithm construction, a discrete laser reflector is composed of a single sharp reflecting surface that results in lidar elevation measurements at a consistent accuracy that is not a function of variation in peak laser reflectance. Further, in the design of our proposed LFSR algorithm, the peak amplitude of the backscattered laser waveform is used as a proxy for coastal landscape characteristics that control the discreteness of laser reflection.

In a test of LFSR algorithm performance within a test site on the North Carolina Outer Banks in the vicinity of the U.S. Army Corps of Engineers Duck Field Research Facility, obvious natural or constructed bald surfaces were correctly classed as fiducial. Landward areas within the test site covered by relatively tall and dense oceanside shrub were mapped as non-fiducial, but much of the salt-spray pruned shrub (personal communication, W. Birkemeier) that exists immediately adjacent to the lee side of the primary dune acts as a fiducial surface for lidar elevation measurement. This result suggests that NASA ATM lidar surveys can detect gradation in shrub canopy closure driven by strong gradients in the physical environment that are commonly observed across barrier islands. The LFSR algorithm is not reliable at locations where spurious elevation differences between repeat topographic lidar surveys are caused by relative horizontal error in laser shot positioning about abrupt changes in relief.

Acknowledgments

The authors thank J. Yungel, A. Waller, J. Sonntag, E. Fredrick, and S. Manizade of EG&G at NASA/GSFC Wallops Flight Facility for their role in the acquisition and processing of the lidar data used in this study. T. Reiss, C. Hapke, and R. Peterson of the USGS Coastal Marine Geology Program contributed to this work by acquiring the ground survey data and aerial photography at Duck, North Carolina, and through assistance in the analysis of the ground and aerial observations. We are also grateful to M. Finn and J. Hagen of the NOAA Aircraft Operations Center for their professionalism and enthusiasm in piloting the aircraft used for the aerial surveys. The USGS Coastal and Marine Program of the Geologic Division funded this work as a component of the National Coastal Change Hazards Project.

References

Blackburn, G.A., and C.M. Steele, 1999. Towards the remote sensing of mattoral vegetation physiology: Relationships between spectral reflectance, pigment, and biophysical characteristics of semiarid bushland canopies, *Remote Sensing of Environment*, 70:278–292.

Blair, J.B., D.B. Coyle, J.L. Bufton, and D.J. Harding, 1994. Optimization of an airborne laser altimeter for remote sensing of vegetation and tree canopies, *Proceedings, International Geoscience and Remote Sensing Symposium '94, Surface and Atmospheric Remote Sensing: Technologies, Data Analyses and Interpretation*, 08–12 August, Pasadena, California, 2:939–941.

Blair, J.B., D.L. Rabine, and M.A. Hofton, 1999. The laser vegetation imaging sensor: A medium-altitude, digitisation-only, airborne laser altimeter for mapping vegetation and topography, *ISPRS Journal of Photogrammetry and Remote Sensing*, 54:115–122.

Brock, J.C., A.H. Sallenger, W.B. Krabill, R.N. Swift, S.S. Manizade, A. Meredith, M. Jansen, and D. Eslinger, 1999. Aircraft laser altimetry for coastal process studies, *Proceedings of the 4th International Symposium on Coastal Engineering and Science of Coastal Sediment Processes*, 21–23 June, Hauppauge, New York, 3:2414–2428.

Brock, J.C., C.W. Wright, A.H. Sallenger, W.B. Krabill, and R.N. Swift, in press. Basis and methods of NASA Airborne Topographic Mapper lidar surveys for coastal studies, submitted to the *Journal of Coastal Research*.

Carter, W.E., and R.L. Shrestha, 1997. Airborne laser swath mapping: Instant snapshots of our changing beaches, *Proceedings of the International Conference on Remote Sensing for Marine and Coastal Environments*, 17–19 March, Orlando, Florida (Environmental Research Institute of Michigan), pp. 298–307.

Ehrenfeld, J.G., 1990. Dynamics and processes of barrier island vegetation, *Aquatic Sciences*, 2(3–4):437–480.

Gutelius, W., J. Green, and D. Carswell, 1997. Application of the Airborne Laser Terrain Mapping System (ALTM) to coastal zone topographic measurement, *Proceedings of the International Conference on Remote Sensing for Marine and Coastal Environments*, 17–19 March, Orlando, Florida (Environmental Research Institute of Michigan), 2:365.

Gutierrez, R., J.C. Gibeaut, M.M. Crawford, M.P. Mahoney, S. Smith, W. Gutelius, D. Carswell, and E. MacPherson, 1998. Airborne laser swath mapping of Galveston Island and Bolivar Peninsula, Texas, *Proceedings of the Fifth International Conference on Remote Sensing for Marine and Coastal Environments*, 05–07 October, San Diego, California, 1:236–243.

Hampton, M.A., J.R. Dingler, A.H. Sallenger, and B.M. Richmond, 1999. Storm-related change of the northern San Mateo County coast, *Proceedings of the 4th International Symposium on Coastal Engineering and Science of Coastal Sediment Processes*, 21–23 June, Hauppauge, New York, 2:1311–1323.

Hapke, C.J., and B.M. Richmond, 1999. The development of a Coastal Aerial Mapping System (CAMS) and its application to the study of coastal morphodynamics, *Proceedings of the 4th International Symposium on Coastal Engineering and Science of Coastal Sediment Processes*, 21–23 June, Hauppauge, New York, 3:2398–2413.

———, 2000. Monitoring beach morphology changes using small-format aerial photography and digital softcopy photogrammetry, *Environmental Geosciences*, 7(1):32–37.

Harris, R.L., G.F. Levy, and J.E. Perry, 1983. *Reevaluation of Vegetational Characteristics at the CERC Field Research Facility, Duck, North Carolina*, Miscellaneous Report No. 83-4, U.S. Army Corps of Engineers, Fort Belvoir, Virginia, 127 p.

Huising, E.J., and E.M.J. Vaessen, 1997. Evaluating laser scanning and other techniques to obtain elevation data on the coastal zone, *Proceedings of the International Conference on Remote Sensing for Marine and Coastal Environments*, 17–19 March, Orlando, Florida (Environmental Research Institute of Michigan), pp. 510–517.

Krabill, W.B., J.G. Collins, L.E. Link, R.N. Swift, and M.L. Butler, 1984. Airborne laser topographic mapping results. *Photogrammetric Engineering & Remote Sensing*, 50(6):685–694.

Krabill, W.B., C.W. Wright, R.N. Swift, E.B. Fredrick, S.S. Manizade, J.K. Yungel, C.F. Martin, J.G. Sonntag, M. Duffy, W. Hulslander, and J.C. Brock, 2000. Airborne Laser Mapping of Assateague National Seashore Beach, *Photogrammetric Engineering & Remote Sensing*, 66(1):65–71.

Kraus, K., and N. Pfeifer, 1998. Determination of terrain models in wooded areas with airborne laser scanner data, *ISPRS Journal of Photogrammetry and Remote Sensing*, 53:193–203.

Lefsky, M.A., W.B. Cohen, S.A. Acker, G.G. Parker, T.A. Spies, and D. Harding, 1999a. Lidar remote sensing of the canopy structure and biophysical properties of Douglas-fir western Hemlock forests, *Remote Sensing of Environment*, 70:339–361.

Lefsky, M.A., D. Harding, W.B. Cohen, G. Parker, and H.H. Shugart, 1999b. Surface lidar remote sensing of basal area and biomass in deciduous forests of eastern Maryland, USA, *Remote Sensing of Environment*, 67:83–98.

Levy, G.F., 1976. *Vegetative Study of the Duck Field Research Facility, Duck, North Carolina*, Miscellaneous Report No. 76-6, U.S. Army Corps of Engineers, Fort Belvoir, Virginia, 80 p.

McDonald, A.J., F.M. Gemmell, and P.E. Lewis, 1999. Investigation of the utility of spectral vegetation indices for determining information in coniferious forests, *Remote Sensing of Environment*, 66:250–272.

Means, J.E., S.A. Acker, D.J. Harding, J.B. Blair, M.A. Lefsky, W.B. Cohen, M.E. Harmon, and W.A. McKee, 1999. Use of large-footprint scanning airborne lidar to estimate forest stand characteristics in the western Cascades of Oregon, *Remote Sensing of Environment*, 67:298–308.

Mish, F.C. (editor), 1989. *Webster's Ninth New Collegiate Dictionary*, Merriam-Webster Inc., Publishers, Springfield, Massachusetts, 1563 p.

Morton, R.A., in press. Factors controlling storm impacts on coastal barriers and beaches—A preliminary basis for real-time forecasting, submitted to the *Journal of Coastal Research*.

Nelson, R., W. Krabill, and G. Maclean, 1984. Determining forest canopy characteristics using airborne laser data, *Remote Sensing of Environment*, 15:201–212.

Ritchie, J.C., 1995. Airborne laser altimeter measurements of landscape topography, *Remote Sensing of Environment*, 53:91–96.

Sallenger, A.H., 2000. Storm impact scale for barrier islands, *Journal of Coastal Research*, 16:890–895.

Sallenger, A.H., W.B. Krabill, J.C. Brock, R.N. Swift, M. Jansen, S. Manizade, B. Richmond, M. Hampton, and D. Eslinger, 1999. Airborne laser study quantifies El Nino-induced coastal change, *EOS, Transactions, American Geophysical Union*, 80(8):80, 92–93.

Zilkoski, D.B., J.H. Richards, and G.M. Young, 1992. Special Report—Results of the general adjustment of the North American vertical datum of 1988, *Surveying and Land Information Systems*, 52(3):133–149.

(Received 24 July 2000; accepted 27 October 2000; revised 23 March 2001)

Attention Students:

ASPRS is pleased to offer five awards totaling more than $11,000. Available to both undergraduate and graduate student-members of ASPRS, these resources have been generated with the intention of advancing academic and professional goals within the fields of Photogrammetry and Remote Sensing. ASPRS recognizes that ***you*** are the future of this rapidly evolving field and hopes you will consider taking advantage of these unique opportunities.

Awards are available in the form of travel grants, cash awards, internship stipends, and data. You must be enrolled in an accredited college or university, and *you must be a member of ASPRS* to be considered. All awards require samples of your work and research goals as part of your application, and that you submit a report to ASPRS outlining your research accomplishments upon completion of your grant period.

LH Systems Internship

The internship provides the award winner with an opportunity to carry out a small research project of his/her own choice, or to work on an existing LH Systems project as part of a team. The award is an eight-week internship for graduate students in photogrammetry. The selected intern will work with LH Systems personnel in LH Systems facilities in San Diego, Denver, Heerbrugg, or elsewhere. The internship consists of a stipend of $2,500 plus an allowance for travel and living expenses for the period of the internship.

Open to graduate students in photogrammetry and remote sensing who are also members of ASPRS.

William A. Fischer Memorial Scholarship

This award is given to facilitate graduate-level studies and career goals adjudged to address new and innovative uses of remote sensing data/techniques that relate to the natural, cultural, or agricultural resources of the Earth. The award consists of a one-year scholarship in the amount of $2,000 and a certificate.

The award is intended for a student who is currently pursuing graduate-level studies or who plans to enroll in a graduate program in an accredited college or university in the U.S. or elsewhere.

Ta Liang Memorial Award

The purpose of this award is to facilitate research-related travel by outstanding graduate students in remote sensing. Such travel includes field investigations, agency visits, participation in conferences, or any travel that enhances or facilitates a graduate research program. The award consists of a grant of $500 and a certificate.

The award is restricted to members of ASPRS who are currently pursuing graduate-level studies in an accredited college or university.

Robert E. Altenhofen Memorial Scholarship

This award is given to encourage and commend college students who display exceptional interest and ability in the theoretical aspects of photogrammetry. The award consists of a cash prize of $2,000 and a certificate.

The award is given to an undergraduate or graduate student, in an accredited college or university, who is a member of ASPRS.

Space Imaging Award for Application of Digital Landsat TM Data

The purpose of this award is to support remote sensing education and stimulate the development of applications of digital Landsat Thematic Mapper (™) data through the granting of digital Landsat data for applied research by undergraduate or graduate students. The award consists of a grant of data valued at up to $4,000, and a plaque inscribed with the recipient's name and that of his/her institution.

The award is given to any undergraduate or graduate ASPRS student member who is enrolled full-time at an accredited college or university with image processing facilities appropriate for conducting the proposed work.

Complete instructions and application forms are available from ASPRS at www.asprs.org or by mail.
The deadline for applications is December 3, 2001.